Stability and targeting of proICA512/IA-2 to insulin secretory granules requires β4-sheet mediated dimerization of its ectodomain in the endoplasmic reticulum

Juha M. Torkko[1,2], M. Evangelina Primo[3,4,*], Ronald Dirkx[1,2], Anne Friedrich[1,2], Antje Viehrig[1,2], Elisa Vergari[1,2], Barbara Borgonovo[1,6], Anke Sönmez[1,2], Carolin Wegbrod[1,2], Martina Lachnit[1,2], Carla Münster[1,2], Mauricio P. Sica[4,5,*], Mario R. Ermácora[4,5], Michele Solimena[1,2,6,#].

[1]Paul Langerhans Institute Dresden, Uniklinikum Carl Gustav Carus, TU Dresden; [2]German Center for Diabetes Research (DZD e.V.); [3]University of Buenos Aires; [4]Instituto Multidisciplinario de Biología Celular, Consejo Nacional de Investigaciones Científicas y Técnicas, [5]Departamento de Ciencia y Tecnología, Universidad Nacional de Quilmes; [6]Max Planck Institute of Molecular Cell Biology and Genetics, Dresden.

Running title: Dimerization of proICA512/IA-2 ectodomain in the ER

[#]To whom correspondence should be addressed: Michele Solimena, Paul Langerhans Institute Dresden, Fetscherstrasse 74, 01307 Dresden, Germany; e-mail: michele.solimena@tu-dresden.de.

[*]Present address: M. E. Primo, Instituto de Immunologigia y Parasitologia, EEA, Instituto Nacional de Tecnología, Agropecuaria-Conicet and M. P. Sica, Laboratorio de Bioenergías, IEDS, Conicet.

Word count for the Materials and Methods: 1,272

Word count for the Introduction, Results and Discussion: 4,099

Molecular and Cellular Biology

ABSTRACT

The type-1 diabetes autoantigen ICA512/IA-2/RPTPN is a receptor protein tyrosine phosphatase of the insulin secretory granules, which regulates the size of granule stores, possibly via cleavage/signaling of its cytosolic tail. The role of its extracellular region, instead, remains unknown. Structural studies indicated that β2- or β4-strands in the mature ectodomain (ME ICA512) form dimers *in vitro*. Here we show that ME ICA512 prompts proICA512 dimerization in the endoplasmic reticulum. Perturbation of ME ICA512 β2-strand N-glycosylation upon S508A replacement allows for proICA512 dimerization, *O*-glycosylation, targeting to granules and conversion, which are instead precluded upon G553D replacement in the ME ICA512 β4-strand. S508A/G553D or N506A/G553D double mutants dimerize, but remain in the endoplasmic reticulum. Removal of the N-terminal fragment (ICA512-NTF) preceding ME ICA512 allows instead an ICA512-ΔNTF G553D mutant to exit the endoplasmic reticulum and ICA512-ΔNTF is constitutively delivered to the cell surface. The signal for SG sorting is located within the NTF RESP18-homology domain (RESP18-HD), whereas soluble NTF is retained in the endoplasmic reticulum. Hence, we propose that the ME ICA512 β2-strand fosters proICA512 dimerization until NTF prevents N506 glycosylation. Removal of this constraint allows for proICA512 β4-strand induced dimerization, exit from the endoplasmic reticulum, *O*-glycosylation and RESP18-HD-mediated targeting to granules.

INTRODUCTION

Receptor protein tyrosine phosphatases (RPTPs) form a large family of transmembrane proteins, which counteract protein tyrosine kinases, and are therefore involved in many signaling pathways. Dimerization of RPTPs is regarded as a main mechanism to regulate their constitutive intracellular phosphatase activity. The contribution of extracellular, transmembrane and cytoplasmic PTP regions to dimerization varies among different RPTPs (1-4).

The extracellular domains of RPTPs can promote the receptor dimerization in several ways. As for receptor protein tyrosine kinases, RPTP oligomerization and clustering can be induced upon heterophilic binding to extracellular ligands. RPTPs for which such mechanism has been demonstrated include the type I RPTP CD45/RPTPC, the type IIa RPTPσ, the type III RPTPβ and the type V RPTPζ (5). In the case of CD45 and RPTPβ changes in their glycosylation pattern, including *O*-glycosylation, were shown to modulate their binding to galectin-1, conceivably increasing clustering and affecting phosphatase activity (6, 7). Homophilic interactions among ectodomains of RPTPs in the same or apposing cells, as it is the case for the type IIb RPTPμ and RPTPκ or the type IV RPTPα, likely represent another mechanism for inducing receptor oligomerization and regulating phosphatase activity (8-10).

The type VII RPTPs ICA512/IA-2/PTPRN and its homologue phogrin/IA-2β/PTPRN2 are 'pseudophosphatases' with a large ectodomain followed by a transmembrane region and a single catalytically inactive PTP domain (11, 12). They are mainly expressed in neuropeptidergic neurons and peptide-secreting endocrine cells,

including insulin producing pancreatic β cells, where they are enriched in secretory granules (SGs) (13, 14). Upon expression in *Escherichia coli* the transmembrane regions of phogrin and ICA512 showed only weak or no ability to interact (2). On the other hand, in transfected fibroblasts the cytosolic juxtamembrane and PTP domains of ICA512 and phogrin were shown to form homodimers as well as heterodimers with each other and with the PTP domains of other conventional RPTPs, possibly inhibiting their phosphatase activity (15). In insulinoma cells, homodimerization of the ICA512 PTP domain was found to disrupt the interaction of the latter with the cortical actin cytoskeleton, thereby affecting insulin SG dynamics and exocytosis (16).

Recent structural studies on the membrane-proximal, recombinant mature, ectodomain of ICA512 (ME ICA512/IA-2), which results from cleavage of proICA512 by prohormone convertases during SG maturation (13, 17), show that this region readily adopts various dimeric assemblies both in the protein crystals and in solution (18, 19). In contrast, the corresponding recombinant mature ectodomain of phogrin, despite its structural similarity to ICA512 (20, 21), was found to fold as a monomer in solution (20, 21). In this study, therefore, we investigated the ability of ME ICA512 to induce receptor homodimerization in insulin-producing cells.

MATERIALS AND METHODS

Generation of ICA512 constructs and site-directed mutagenesis. pEGFP-N1 constructs encoding full length human ICA512 (amino acids 1-979), ICA512 N-terminal fragment (NTF, amino acids 35-446), ICA512 ΔNTF (amino acids 449-979), ICA512 Regulated endocrine-specific protein 18 homology domain (RESP18-HD, amino acids 35-131) or ME (amino acids 449-575) were fused at their C-termini to green fluorescent protein (GFP) or a hemagglutinin (HA) epitope tag. These constructs included either the native signal peptide or that of CD33, while an 11-mer linker was placed between ME ICA512 and GFP. Conventional cloning strategies were also used to generate ICA512-NTF or a secretory GFP by inclusion of the CD33 signal peptide at the N-terminus. Site-directed mutagenesis, using these constructs as template, was performed with the QuikChange™ kit (Stratagene). All constructs and mutations were verified by sequencing.

Antibodies against ICA512-NTF, ME ICA512, and ICA512 CT. Mouse monoclonal antibodies directed against a recombinant fusion protein between GST and amino acids 389-575 (anti-ectodomain) or amino acids 935-974 (anti-ICA512 cytoplasmic tail; CT) of human ICA512 were generated in the Antibody Facility at the Max Planck Institute of Molecular Cell Biology and Genetics (MPI-CBG, Dresden, Germany). The ectodomain antibodies were further selected for recognition of an epitope within amino acids 389-446 of the NTF (anti-ICA512 NTF ab) or amino acids 449-575 of ME ICA512 (anti-ME ICA512 ab) using a MesoScale Discovery platform and by Western blotting against ICA512-NTF-GFP, ICA512-GFP ΔNTF and GST.

Culture and transfection of insulinoma INS-1 cells. Rat INS-1 cells were grown in RPMI 1640 medium as described (22). Cells were split every 4-days, plated onto coverslips on 35 mm dishes (Costar® 3516) and transfected 3 days after with plasmid-DNA diluted into Cytoporation^{R} medium using Cyto Pulse electroporator (Cyto Pulse Sciences, Inc.). Four days after transfection, cells were pre-incubated for 1 hour in resting buffer (5 mM KCl, 120 mM NaCl, 24 mM $NaHCO_3$, 1 mM $MgCl_2$, 2 mM $CaCl_2$, 1 mg/ml ovalbumin, 5 mM HEPES pH 7.5) and then either kept at rest or in stimulation buffer [25 mM glucose (high glucose, HG) and 55 mM KCl (high K^+, HK) in 70 mM NaCl, 24 mM $NaHCO_3$, 1 mM $MgCl_2$, 2 mM $CaCl_2$, 1 mg/ml ovalbumin, 5 mM HEPES pH 7.5] for additional 2 hours. In some instances, 30 µM Calpeptin or MG-115 (Calbiochem) was added to the stimulation buffer. After 2 hours of incubation, cells were washed twice with ice-cold PBS and harvested in ice-cold lysis buffer [(20 mM Tris-Cl pH 8.0, 140 mM NaCl, 1 mM EDTA, 1 mM Triton X-100 and 1% protease inhibitor cocktail (Sigma P8340)]. Cell lysates were centrifuged at 4°C 12,000 rpm for 5 min in an Eppendorf 5415C centrifuge. The pre-cleared soluble protein fraction was separated from the pellet and prepared in SDS-PAGE sample buffer for Western blotting analysis.

Immunoprecipitation (IP). Equal amount of cell lysates were mixed with 20 µl (1/10 vol/vol) Protein G Sepharose beads (GE Healthcare), and incubated on a rotating wheel at 4°C for 30 min to pre-clear the lysates of the IgG bound protein fraction. The lysates were centrifuged at 2,000 rpm for 3 min in the Eppendorf centrifuge and the pellet of beads removed. Goat anti-GFP antibodies (MPI-CBG, Dresden, Germany) or IgG from goat serum (Sigma I5256), 1:100-dilution, respectively, were then incubated with the pre-cleared lysates overnight prior to the addition of 20 µl (1/10 vol/vol) Protein G

Sepharose beads. The lysates were centrifuged at 2,000 rpm for 3 min and the soluble fraction was removed. The beads were washed twice with PBS, centrifuged as above and re-suspended in SDS-PAGE sample buffer for Western blotting analysis.

Enzymatic de-glycosylation assays. INS-1 cells transfected for expression of different ICA512 variants, or mouse or human islet cells, were incubated in resting or stimulation buffer for 2 hours. Cells were lysed as above and incubated in denaturation buffer (New England Biolabs) at 95°C for 5 min. The denatured samples of the cell lysates were then incubated with PNGaseF, Endoglycosidase H or *O*-glycosidases, endo-α-N-acetylgalatosaminidase and neuramidase in 1x reaction buffer (New England Biolabs) at 37°C for 3 hours. Glycosylated fetuin from fetal calf serum (Sigma F2379) was used as a control to confirm the performance of glycosidases. Non- and enzyme-treated cell lysates were prepared in SDS-PAGE sample buffer for Western blotting analysis.

Western blotting. Cell lysates and IPs in SDS-PAGE sample buffer were heated to 95°C for 5 min, and then subjected to SDS-PAGE and Western blotting. The following primary antibodies were employed: mouse monoclonal anti-GFP antibody (Clontech #632381); mouse anti-ICA512 antibody, HM-1 (23); mouse anti-γ-tubulin antibody (Sigma T6557) and rabbit anti-HA antibody (Abcam ab9110). Primary antibodies were detected with goat anti-mouse or anti-rabbit HRP-conjugated IgGs (Bio-Rad) followed by addition of substrates for chemiluminescence (Thermo Scientific, Pierce Biotechnology) and a LAS-3000 Imaging System (Fuji). Black dividing lines indicates cutting of the same or different Western blots or their groupings.

Immunostaining and confocal microscopy. INS-1 cells transfected for the expression of different ICA512 variants and grown on coverslips on 35 mm dishes for 4 days post-transfection were incubated in resting or stimulation buffer as described above, then rinsed 3x in PBS and fixed with 4% paraformaldehyde. After aldehyde quenching and permeabilization (200 mM glycine, 0.1% Triton X-100 in PBS) for 20 min, cells were incubated in blocking buffer (0.2% Gelatin, 0.5% albumin in PBS) for 1 hour, and thereafter in blocking buffer with guinea pig anti-insulin antibody (Abcam ab7842) or rabbit anti-calnexin antibody (Sigma C4731) at 4°C overnight. Next, cells were washed 5x with PBS, and then incubated in blocking buffer with goat anti-guinea pig or anti-rabbit AlexaFluor568-conjugated IgGs (Molecular Probes) for 2 hours at room temperature. After additional washing 5x with PBS, immunolabeled coverslips were mounted onto slides with Mowiol™.

INS-1 live cell staining with the ER tracker red dye (glibenclamide BODIPY®TR; Molecular Probes) was done according to the manufacturer's protocol. ICA512 mature ectodomain or cytosolic domain specific antibodies (see above), the anti-ME ICA512 antibody or the anti-ICA512 CT antibody was incubated with living INS-1 cells to assess ICA512 extracellular domain exposure at the cell surface. Images of labeled cells were acquired with an Olympus FluoView-1000 laser scanning confocal microscope equipped with a 60x PlanoApo OLSM lens (NA=1.10).

Cell sorting. Four days post-transfection with ICA512-GFP, ICA512-GFP G553D or ICA512-GFP N506A/N524A cells were detached by trypsin digestion and re-suspended in 1x PBS, 25 mM HEPES (pH 7.0), 1 mM EDTA and 1% albumin. The cell suspension was filtered through cell-strained cap in 5 ml round-bottom Falcon® tubes (Corning

352235) prior to sorting for GFP expression with a Becton Dickinson BD FACS Aria II. Sorted cells expressing the ICA512-GFP variants were cultured in 24 mm culture dishes (Costar® 3513) in RPMI 1640 medium.

Insulin gene expression, contents and secretion. After two days in culture, the total RNA of $1x10^5$ cells sorted for the expression of each ICA512-GFP variant was purified with Qiagen RNeasy Kit and used as RNA template for the First-Strand cDNA synthesis with SuperScript™ II reverse transcriptase (Invitrogen) and oligo (dT) primer. Levels of insulin mRNA were analysed by Quantitative real-time PCR with the qPCR GoTaq kit (Promega) and an MX4000 Thermocycler (Stratagene). β-actin mRNA was amplified in parallel for normalization of the insulin mRNA levels in the individual samples. Alternatively, $3x10^5$ ICA512-GFP$^+$ sorted cells were switched to resting buffer for pre-incubation for 1 hour and then to resting or stimulation buffer for additional 2 hours before being harvested for analyses for proinsulin/ insulin content and insulin secretion in static conditions with Rat/Mouse Proinsulin/ Rat Insulin ELISA (Mercodia).

Statistical analysis. All data are representative of three or more independent experiments, with the exception of the analysis in human islets, which was performed two times. Statistical significance was assessed with student's T-test or ANOVA.

RESULTS

ProICA512 dimerizes in INS-1 cells. ME ICA512 encompasses amino acids 449-575 of human ICA512 (Fig. 1A). The X-ray structure of recombinant ME ICA512 (Fig. 1B) (18) encompassing amino acids 468-558 revealed that this region displays a ferredoxin-like fold related to the SEA (sea urchin sperm protein, enterokinase, agrin) domain, which is known to promote oligodimerization (24-28). Accordingly, both crystallized (18) and soluble (19) ME ICA512 form dimers resulting from the antiparallel pairing of β2-β2 or β4-β4 strands (Fig. 1B) (19).

To verify the occurrence of ICA512 dimers in insulin-producing cells, full-length ICA512 constructs differentially tagged at their C-termini with GFP (ICA512-GFP) or a HA epitope (ICA512-HA) (Fig. 2A) were transiently expressed alone or together in rat insulinoma INS-1 cells. Consistent with previous findings (29, 30), the mature transmembrane fragments (TMF) of ICA512-GFP (ICA512-TMF-GFP; ~100 kDa) and ICA512-HA (ICA512-TMF-HA; ~75 kDa) were the major ICA512 species detected in cell lysates of resting (R) INS-1 cells (Fig. 2A). In cells stimulated (S) with 25 mM glucose with or without 55 mM KCl, the respective proICA512 species became the most prominent species, while the levels of the corresponding ICA512-TMF, which undergo calpain mediated cleavage upon SG exocytosis (29, 30), were drastically reduced. Stimulation with 55 mM KCl alone, which prompts SG exocytosis, reduced also the levels of ICA512-TMF, but barely up-regulated those of proICA512. The detection of multiple proICA512 species reflects the different degree of glycosylation of the protein during its maturation along the secretory pathway prior to cleavage and conversion into

ICA512-TMF. Notably, in cells stimulated with 55 mM KCl alone, the major proICA512 form migrated faster than the proICA512 species detected in cells concomitantly exposed to high glucose. This discrepancy conceivably reflects differences in the efficiency of proICA512 N-glycosylation in the endoplasmic reticulum (ER) depending on the glucose levels.

ProICA512-HA and ICA512-TMF-HA were readily detectable, albeit at lower levels when co-expressed with ICA512-GFP (Fig. 2B). Immunoprecipitation with anti-GFP antibodies led to the recovery of ICA512-TMF-GFP or proICA512-GFP from resting or stimulated cells, respectively (Fig. 2C, top panel). Co-immunoprecipitation of proICA512-HA, but not of ICA512-TMF-HA, suggests that proICA512, but not ICA512-TMF form dimers (Fig. 2C, bottom panel). Neither ICA512-GFP nor ICA512-HA co-immunoprecipitated with control IgGs.

ME ICA512 mediates the dimerization of proICA512 in INS-1 cells. Previous studies *in vitro* and in transfected INS-1 cells indicated that the intracellular PTP domain of ICA512 can dimerize (15, 16). To verify whether ME ICA512 could account for proICA512 dimerization independently of the cytoplasmic domain, INS-1 cells were transfected with ICA512-HA either alone or in combination with soluble ME ICA512-GFP (Fig. 2D, left panel). The slowest electrophoretic species of ME ICA512 was upregulated in stimulated cells and migrated at the expected size of ca. 50 kDa, taking into account also its N-glycosylation. The fastest migrating species corresponds instead to the non-glycosylated form of ME ICA512-GFP (see also below, Fig. 5D). Immunoprecipitation of ME ICA512-GFP led to the specific recovery of proICA512-HA from both resting and stimulated cells (Fig. 2D, right panel). Hence, consistent with *in*

vitro structural and biochemical analyses (18, 19), ME ICA512 is sufficient to induce the dimerization of proICA512 in INS-1 cells.

Lack of N-glycosylation or perturbation of the β2-β2 association interface of ME ICA512 do not preclude SG sorting and conversion of ICA512. Electrophoretic mobility shift of ICA512 upon digestion with PNGaseF indicated that the protein is N-glycosylated (17, see also below Fig. 4C and 8D). ICA512 contains only two consensus sites for N-glycosylation at N506 and N524, both within ME ICA512 (Fig. 1A and 1B). N506 is located in the β2-strand (Fig. 1B), a critical structural element for β2-β2 dimerization (19). The consensus sequence for N506 glycosylation includes S508, which was shown to mediate β2-β2 dimerization of ME ICA512 *in vitro* (19). N524 is instead remote from the identified dimerization interfaces (Fig. 1B).

To verify the glycosylation of both N506 and N524, INS-1 cells were independently transfected with the single mutants ICA512-GFP N506A, ICA512-GFP S508A and ICA512-GFP N524A, or with the double mutant ICA512-GFP N506A/N524A. ICA512-TMF of all ICA512-GFP mutants, as detected with the anti-GFP or the anti-ICA512 HM-1 antibody, displayed a faster electrophoretic mobility than wild type ICA512 in resting cells (Fig. 3A). A similar behavior was observed for the corresponding proICA512-GFP species in resting and stimulated cells (Fig. 3A and 3B). Thus, both N506 and N524 are glycosylated. The expression of proICA512-GFP N506A/N524A was significantly higher than that of ICA512-GFP or single N-glycosylation ICA512-GFP mutants (Fig. 3C), conceivably due to its delayed folding, traffic and conversion. Lack of N-glycosylation, however, did not prevent the sorting of ICA512-GFP N506A/N524A into SGs, as indicated by its co-localization with insulin at the cell periphery of INS-1 cells similar to

ICA512-GFP (Fig. 3D). Notably, ICA512-GFP S508A, in which the β2-β2 dimerization should be perturbed (19), was also sorted into SGs (Fig. 3D).

The total levels of insulin mRNA in ICA512-GFP N506A/N524A^{+} sorted cells was not significantly changed compared to ICA512-GFP^{+} sorted cells (Fig. 3E). Likewise, in ICA512-GFP N506A/N524A^{+} sorted cells the proinsulin (Fig. 3F) and insulin (Fig. 3G) content as well as the fractional stimulated insulin secretion (Fig. 3H) were not significantly reduced compared to ICA512-GFP^{+} sorted cells.

Perturbation of the ME ICA512 β4-β4 association interface precludes SG sorting and conversion of ICA512. The replacement of G553, which sterically and electrostatically hinders β4-β4 dimerization (19), differently from the replacement of N506 or S508 in the β2-β2 interface, profoundly altered the maturation and stability of ICA512. Specifically, the expression of ICA512-TMF-GFP G553D was dramatically reduced (Fig. 4A and 4B, lane 4). This was also the case upon cell treatment with the proteasome inhibitor MG-115 (Fig. 4A, lane 6) or calpeptin (Fig. 4B lane 6), which prevents the calpain-mediated cleavage of ICA512-TMF and thus its disappearance (Fig. 4B, lane 3). These observations suggested that the G553D replacement prevents the conversion of proICA512-GFP into ICA512-TMF-GFP. Conversely, expression of ICA512-GFP G553D correlated with the enrichment of proteolytic fragments, mostly in resting cells (Fig. 4A and 4B, lanes 1 and 4), but also in stimulated cells treated with MG-115 (Fig. 4A, lanes 3 and 6) or calpeptin (Fig. 4B, lanes 3 and 6). Notably, proICA512-GFP G553D appeared as a single band with electrophoretic mobility comparable to the fastest migrating species of proICA512-GFP (Fig. 4A and 4B, lane 2 vs. 5). Sensitivity to PNGaseF treatment indicated, that this phenotype is not attributed to lack of N-

292 glycosylation (Fig. 4C). Analysis by confocal microscopy further indicated that ICA512-
293 GFP G553D (Fig. 4D left panel), unlike ICA512-GFP and ICA512-GFP S508A (Fig.
294 3D), did not co-localize with insulin (Fig. 4D, left panel), but was dispersed throughout
295 the cytoplasm with a reticular pattern resembling that of ER tracker red dye (Fig. 4D,
296 right panel). These data suggested that ICA512-GFP G553D is retained within the ER.
297 In ICA512-GFP G553D^{+} sorted cells, similar to ICA512-GFP N506A/N524A^{+} sorted
298 cells (see above, Fig. 3), the total levels of insulin mRNA was not changed (Fig. 4E). The
299 proinsulin (Fig. 4F) and insulin content (Fig. 4G) as well as the fractional stimulated
300 insulin release (Fig. 4H) were also not significantly changed relative to ICA512-GFP^{+}
301 sorted cells.
302 **ICA512 is *O*-glycosylated.** ME ICA512 possesses a SEA domain fold, which is
303 present in some mucins and other membrane proteins. SEA domain containing proteins
304 are commonly extensively *O*-glycosylated nearby this domain, possibly to hinder its
305 proteolysis (25, 27, 28). We wondered therefore, whether ICA512 is also *O*-glycosylated
306 and whether this modification, which mainly occurs in the Golgi, would be affected by
307 the G553D replacement.
308 *O*-glycosidase treatment increased the electrophoretic mobility of the *O*-glycosylated
309 control protein fetuin (Fig. 5A), as well as that of ICA512-TMF-GFP in extracts of
310 resting cells (Fig. 5B, lane 1 vs. 2). De-*O*-glycosylation of lysates from stimulated cells
311 led to the almost complete disappearance of the slowest migrating species of proICA512-
312 GFP (Fig. 5B, lane 3 vs. 4). A comparable mobility shift of ICA512-TMF was observed
313 upon *O*-glycosidase treatment of lysates of mouse and human islets (Fig. 5C), thus
314 indicating that this modification, similar to N-glycosylation (17), occurs also in non-

transformed ICA512 expressing tissues. ProICA512-GFP N506A (Fig. 5B, lane 5 vs. 6 and lane 7 vs. 8) and proICA512-GFP S508A (Fig. 5B, lane 9 vs. 10 and lane 11 vs. 12), as well as the corresponding ICA512-TMF forms (Fig. 5B, lane 5 vs. 6 and lane 9 vs. 10), were also *O*-glycosidase sensitive. Conversely, the single proICA512-GFP G553D species was *O*-glycosidase insensitive (Fig. 5B, lane 15 vs. 16), consistent with its retention in the ER (Fig. 4D).

Relevance of the NTF domain for *O*-glycosylation and export of proICA512 from ER. Soluble ME ICA512-GFP, ME ICA512-GFP S508A and ME ICA512-GFP G553D (Fig. 5D, lanes 1, 5 and 9) were reduced to a single band upon treatment with N-glycosidases, Endoglycosidase H (Fig. 5D, lanes 2, 6 and 10) or PNGaseF (Fig. 5D, lanes 3, 7 and 11), but were insensitive to *O*-glycosidases (Fig. 5D, lanes 4, 8 and 12). Thus, multiple ME ICA512-GFP species result from N-glycosylation alone. However, the Endoglycosidase H sensitivity of all these ME ICA512 variants further indicated these retain the high-mannose structure N-oligosaccharide chains, *i.e.* they are not exported from the ER. Indeed, confocal microscopy indicated that ME ICA512-GFP or its G553D variant was found to accumulate in the ER (Fig. 5E), concurrent with the lack of *O*-glycosylation.

Sequence analysis of ICA512 with NetOGlyc 3.1 (31) pointed to serines and threonines clustered within amino acid residues 400-440, *i.e.* in the NTF domain (13, 17), preceding ME ICA512, as the most likely sites for *O*-glycosylation (Fig. 1A). Nonetheless, the deletion mutant ICA512-GFP ΔNTF, which lacks amino acid residues 35-448 (Fig. 1A), *i.e.* the entire NTF domain, as well as the corresponding ICA512-GFP ΔNTF S508A and ICA512-GFP ΔNTF G553D mutants, were both PNGaseF (Fig. 5F,

lanes 3, 7 and 11) and *O*-glycosidase (Fig. 5F, lanes 4, 8 and 12) sensitive. Notably, ICA512-GFP ΔNTF and ICA512-GFP ΔNTF G553D displayed comparably slower electrophoretic mobility than ICA512-GFP ΔNTF S508A, suggesting their similar glycosylation at N506 and N524. Moreover, ICA512-GFP ΔNTF G553D, similar to all other constructs lacking NTF, was Endoglycosidase H resistant (Fig. 5F, lanes 2, 6 and 10) and unlike ICA512-GFP G553D did not undergo extensive proteolysis. Evidence that proICA512 mutants lacking NTF domain can fold and exit from the ER, even if the ME ICA512 β4-β4 dimerization interface is perturbed suggests that this region contains information for retention of unfolded proICA512 in the ER.

ICA512-NTF is required for targeting of proICA512 to the SGs. To further verify the progression of ICA512-GFP ΔNTF along the secretory pathway, we imaged its localization in non-permeabilized resting (Fig. 6A and 6B) or stimulated (Fig. 6C) INS-1 cells kept at 4°C to block endocytosis. Both ICA512-GFP and ICA512-GFP ΔNTF, as detected with their GFP fluorescence, appeared enriched at the cell periphery (Fig. 6A, 6B and 6C). However, labeling with a novel mouse anti-ME ICA512 antibody revealed that ICA512-GFP ΔNTF, unlike ICA512-GFP, was exposed at the cell surface even in resting conditions (Fig. 6A). As expected, the concomitant control labeling of resting cells for insulin, which like ICA512-GFP should be mainly confined to SGs and not be exposed at the surface, was negative (Fig. 6A). Surface labeling with a mouse anti-ICA512 CT antibody was also negative (Fig. 6B). Conversely, the anti-ME ICA512 antibody labeled the cell surface of both ICA512-GFP and ICA512-GFP ΔNTF stimulated cells, albeit more prominently in the case of the latter cells (Fig. 6C). Thus, ICA512-GFP ΔNTF, unlike ICA512-GFP, is constitutively targeted to the cell surface.

Immunoblotting with anti-GFP (Fig. 6D) or anti-ME ICA512 (Fig. 6E) antibodies indicated that unlike ICA512-GFP (Fig. 6D and 6E, lanes 1 vs. 2), ICA512-GFP ΔNTF (Fig. 6D and 6E, lanes 3 vs. 4) is not susceptible to Ca^{2+}/calpain-dependent cleavage upon stimulation of INS-1 cells. Hence, the NTF domain is not only required to retain unfolded proICA512 in the ER, but also for targeting the latter to SGs, thus enabling the cleavage of ICA512-TMF upon granule exocytosis (29, 30).

The RESP18 homology domain targets proICA512 to SGs. The most N-terminal portion of ICA512-NTF corresponds to the RESP18 homology domain (RESP18-HD) (32), which begins at amino acid residue 35, following the signal peptide and ends at a putative cleavage site for protein convertases, between residues 133 and 134 (17) (Fig. 1A). Similar to RESP18 (32, 33), ICA512-RESP18-HD is characterized by a cysteine-rich motif (Fig. 1A), which may be relevant for sorting into SGs. In particular, other characteristic neuroendocrine proteins, such as Chromogranin B and Secretogranin II, have been shown to depend on disulfide-bonded loops for their targeting to SGs (34-36).

Consistent with the enrichment of RESP18 in SGs (32, 33), also soluble ICA512-RESP18-HD-GFP co-localized extensively with insulin in SG like structures (Fig. 7A) and its recovery in the media was enhanced upon stimulation of the cells (Fig. 7B). Conversely, soluble ICA512-NTF-GFP, despite the inclusion of the RESP18-HD, rather displayed a diffuse ER like pattern (Figs. 7C and D), resembling that of the ER marker calnexin (Fig. 7D). A similar expression pattern was observed for ICA512-NTF (Fig. 7F), as detected with a novel antibody that recognizes human NTF, but not the equivalent domain of the endogenous rat protein (Fig. 7E, lane 1 vs. 2). These data exclude the possibility that retention of soluble ICA512-NTF in the ER is secondary to its misfolding

upon fusion with GFP. Intriguingly, in cells expressing soluble ICA512-NTF-GFP insulin immunoreactivity was also more diffuse, rather than being enriched in SGs, as in cells expressing ICA512-RESP18-HD-GFP (Fig. 7A). Thus, RESP18-HD contains information that is sufficient for SG targeting, while the remaining portion of ICA512-NTF exerts a dominant role in ER retention, unless associated with the remaining C-terminal transmembrane portion of the protein.

The ME ICA512 β4-β4 strand interface is involved in dimerization. Finally, we investigated in cells the occurrence of the main dimerization modes identified in the X-ray structure of non-glycosylated ME ICA512 (18, 19). The association through a β2-β2 interface was tested by the S508A mutation, which impedes dimerization *in vitro* (albeit not in the crystal) of recombinant non-glycosylated ME ICA512. The second dimerization mode, through the β4-β4 interface, was tested by the G553D replacement, which is sterically incompatible with it (19). ICA512-HA and ME ICA512-GFP variants with the symmetric single or combined mutations were co-expressed in INS-1 cells, and the lysates of the stimulated cells and the corresponding immunoprecipitates were analyzed by immunoblotting (Fig. 8A and 8B). While symmetric replacement of S508 did not preclude the recovery of proICA512-HA S508A with ME ICA512-GFP S508A (Fig. 8B, lane 9), the symmetric replacement of G553 prevented the co-immunoprecipitation of proICA512-HA G553D with ME ICA512-GFP G553D (Fig. 8C, lane 10). The recovery of proICA512-HA mutants with the corresponding ME ICA512-GFP variants was specific, as co-immunoprecipitations with control IgG were significantly less effective compared to those with the anti-GFP antibody (Fig. 8B, lanes 13-18 and Fig. 8C). These findings suggest that dimerization of proICA512 occurs

through β4-β4 interactions. Remarkably, however, the combined replacement of S508A/G553D was still permissive for ME ICA512 dimerization, albeit the recovered proICA512-HA S508A/G553D displayed a faster electrophoretic mobility (Fig. 8B, lane 11), consistent with lack of N506 glycosylation. Hence, even upon perturbation of the β4-β4 interface, the dimerization may still occur via the β2-β2 interaction, but only in conditions which prevent/precede N506 glycosylation. Glycosylation, because of its bulkiness, would impede the physical contact between β2-strands. Consistent with this interpretation was the greater yield of co-immunoprecipitated proICA512-HA upon replacement□□□ N506 rather than S508 □in combination with G553 (Fig. 8B, lane 12 and Fig. 8C).

According to the structural data N506 is less critical than S508 for the establishment/retention of β2-β2 dimer interface (19), and thus for protein folding and stability, as corroborated by the greater amount of proICA512-HA N506A/G553D compared to proICA512-HA S508A/G553D in the cell lysate (Fig. 8A, lane 6 vs. 5). Notably, β2-β2 proICA512 dimers are mainly retained in the ER, as shown in the specific case of proICA512-HA S508A/G553D, which for the most part remains Endoglycosidase H sensitive (Fig. 8D, lower panel) and is not converted into the corresponding mature ICA512-TMF species (Fig. 8D, upper panel). Hence, preclusion of N506 glycosylation does not rescue the replacement of G553, but it allows the detection of β2-β2 mediated dimerization of ME ICA512, which in normal conditions may only represent a transient state of the receptor. Once N506 glycosylation occurs, folding of the β4-β4 interface would become critical for stabilization/dimerization of proICA512 and for overcoming the dominant ER retention signal within ICA512-NTF, thus enabling the further

progression of the protein along the secretory pathway and its RESP18-HD mediated targeting to the SGs (Fig. 8E).

DISCUSSION

Dimerization of RPTPs has been generally found to occur at the cell surface. This process is driven by the interaction of ligands to the extracellular domain and can affect the phosphatase activity of the cytoplasmic PTP domain. In the case of ICA512, however, no extracellular ligands have yet been identified. Its signaling pathway remains also unclear, albeit the calpain cleaved cytosolic fragment generated upon granule exocytosis has been suggested to act as a retrograde signal to modulate insulin SG mobility and biogenesis in relationship to the size and consumption of the SG stores (30, 23, 16). In this work we have began to unravel some of the functional properties of the ICA512 SG luminal/ extracellular region.

Specifically, we show that ME ICA512 is sufficient to promote ICA512 dimerization in cells (Fig. 2D), as suggested by previous structural studies of the corresponding recombinant portion of the receptor (18, 19). Notably, we only detected dimers of proICA512, but not of ICA512-TMF (Fig. 2C and D), implying that maturation of the protein resolves this interaction such that in the SGs ICA512-TMF is present as a monomer. On the other hand we cannot exclude that in the granule lumen ICA512-TMF forms instead a heterodimer with soluble ICA512-NTF generated from convertase-mediated cleavage of proICA512 between residues 448 and 449 (Fig. 1A). Repeated attempts to co-immunoprecipitate ICA512-NTF with ICA512-TMF, however, have been unsuccessful. Since ICA512-NTF contains two additional likely sites for convertase cleavage between residues 133-134 and 387-388 (Fig. 1A), it is also possible that two putative fragments of ~28 kDa and ~7 kDa resulting from these cleavages might have not

been detected on SDS-PAGE and Coomassie blue/silver staining, either being masked by the IgG light chain or due to their small size. Other factors that may disrupt ME ICA512 dimers include post-translational modifications occurring while the protein transits from the ER to the SGs, the progressive intraluminal acidification of the Golgi and SG compartment and/or binding to other secretory proteins. Intriguingly, it has been reported that phogrin/IA-2β interacts with carboxypeptidase E/H (37). Finally, we cannot rule out that ME ICA512 prompts again homodimerization of ICA512-TMF once the latter is transiently inserted into the plasma membrane upon granule exocytosis.

Our data suggest that dimerization of proICA512 occurs in the ER. Supporting this conclusion is the fact that proICA512-GFP G553D accumulates in the ER (Fig. 4D) and does not undergo *O*-glycosylation (Fig. 5B), a post-translation modification that most commonly occurs in the Golgi. However, ICA512-GFP ΔNTF G553D is Endoglycosidase H resistant and *O*-glycosylated (Fig. 5F). These findings together with the evidence that soluble NTF accumulates instead in the ER (Fig. 7C, 7D and 7F), suggest that NTF contains an ER retention signal. In contrast, soluble RESP18-HD-GFP, similar to its paralogue RESP18 (32, 33, 38) is targeted to the SGs (Fig. 7A) and released in a regulated fashion from the cells (Fig. 7B). Accordingly, ICA512-GFP ΔNTF is neither retained in the ER nor targeted to SGs, but constitutively delivered to the cell surface (Fig. 6A-C). Intriguingly, in cells overexpressing soluble NTF, but not soluble RESP18-HD, insulin immunoreactivity is also more diffused and less granular (Fig. 7C). Additional studies on the structure of ICA512-NTF and RESP18-HD and their roles in SG biogenesis will be necessary to elucidate the reason for these phenomena.

Extending previous findings (17, 39, 40), we show that N506 and N524 of ICA512 are both glycosylated (Fig. 3A and 3B). Lack of glycosylation at these sites does not prevent targeting of proICA512 to SGs (Fig. 3D) and its conversion to ICA512-TMF (Fig. 3A). Simultaneous inhibition of N506 glycosylation and perturbation of the ME ICA512 β2-β2 association interface by replacement of S508A is also insufficient to prevent proICA512 conversion to ICA512-TMF (Fig. 3A) and ME ICA512 mediated homodimerization (Fig. 8B). Conversely, perturbation of the ME ICA512 β4-strand by G553D replacement hinders the stability, SG targeting and conversion of proICA512 (Fig. 4A-D), as well as its recovery as a homodimer (Fig. 8B). On the other hand, combined S508A/G553D or N506A/G553D replacements are still compatible with proICA512 dimerization (Fig. 8B). A possible explanation for the latter finding is that the extended β2-β2 association interface (19, Fig. 1A and 1B) is sufficient for stable proICA512 dimerization, provided that glycosylation of N506, as upon S508A replacement, is precluded. This conclusion is corroborated by the greater yield of pro-ICA512 homodimer recovered when the G553D mutation is combined with N506A replacement, which structural studies predict to be less detrimental for ME ICA512 β2-β2 mediated dimerization than S508A replacement (Fig. 8B and 8C). Notably, such β2-β2 mediated proICA512 dimers are restricted to the ER, as indicated by the Endoglycosidase H sensitivity and lack of conversion of proICA512-GFP S508A/G553D (Fig. 8D).

In conclusion, we propose a model whereby proICA512 β2-β2 dimers prevail over β4-β4 dimers in the ER as long as the β2-strand N506 is not glycosylated possibly due to occlusion of this region by NTF. Dislocation of NTF, as upon its binding to another

molecule, would allow for N506 glycosylation, thus irreversibly shifting the equilibrium towards proICA512 β4-β4 dimers, consequently allowing ICA512 to leave the ER (Fig. 8E). Importantly, this model does not assume that β4-β4 dimerization is *per se* the signal for ER export. Indeed, ICA512-GFP ΔNTF G553D, in which concomitant glycosylation of N506 and G553D replacement should hinder with the formation of both ME ICA512 β2-β2 and β4-β4 dimers, is nevertheless exported from the ER, conceivably as a monomer. Hence, it is plausible that folding and/or homodimerization of ME ICA512 β4-strand are instrumental to stabilize proICA512 and overcome the NTF ER retention signal.

ACKNOWLEDGMENTS

We thank Patrick Keller and the MPI-CBG Antibody Facility in Dresden for the help in raising monoclonal antibodies against ICA512, Anja Steffen, Barbara Ludwig and Stephan Bornstein in our University Clinic for the provision of human islets, Torsten Willert and Katja Schneider in the FACS Facility of the CRTD at TU Dresden for cell sorting, all members of the Solimena lab for discussion and Katja Pfriem for excellent administrative assistance.

This work in the Solimena lab was supported by funds from the DFG-SFB 655 and the German Ministry for Education and Research (BMBF) to the German Center for Diabetes Research (DZD e. V.) and the German Clinical Competence Network for Diabetes Mellitus (KKNDm; FKZ:01GI1102). The collaboration between the Solimena and Ermácora groups has been supported by the DFG Exchange Program Germany-Argentina N. 444ARG113/9/1-0. The work in the Ermácora lab was supported by funds from the Consejo Nacional de Investigaciones Cientificas y Técnicas of Argentina (Conicet; PIP-GI 11220090100044), the Agencia Nacional de Promoción Cientifica y Tecnológica of Argentina (ANPCyT; PICT-2010-0580), the Universidad Nacional de Quilmes (UNQ; 53/1002). Dr. J. Torkko has been the recipient of a JDRF Postdoctoral Fellowship Award.

ABBREVIATIONS

ER	endoplasmic reticulum
IP	immunoprecipitation
ME	mature ectodomain
NTF	N-terminal fragment
RESP18	Regulated endocrine-specific protein 18
SG	secretory granule
TMF	transmembrane fragment

542 **REFERENCES**

543

544 1. **Blanchetot C, Tertoolen LG, Overvoorde J, den Hertog J.** 2002. Intra- and
545 intermolecular interactions between intracellular domains of receptor protein-tyrosine
546 phosphatases. J. Biol. Chem. **277:**47263-47269.

547

548 2. **Chin C, Sachs JN, Engelman DM.** 2005. Transmembrane homodimerization of
549 receptor-like protein tyrosine phosphatases. FEBS Lett. **579:**3855-3858.

550

551 3. **Tonks NK. 2006.** Protein tyrosine phosphatases: from genes, to function, to disease.
552 Nat. Rev. Mol. Cell Biol. **7:**833-846.

553

554 4. **Barr AJ, Ugochukwu E, Lee WH, King ON, Filippakopoulos P, Alfano I, Savitsky**
555 **P, Burgess-Brown NA, Muller S, Knapp S.** 2009. Large-scale structural analysis of
556 the classical human protein tyrosine phosphatome. Cell **136:** 352-363.

557

558 5. **Mohebiany AN, Nikolaienko RM, Bouyian S, Harroch S.** 2012. Receptor-type
559 tyrosine phosphatase ligands: looking for the needle in the haystack. FEBS J. **280:**388-
560 400.

561

562 6. **Abbott KL, Matthews RT, Pierce M.** 2008. Receptor tyrosine phosphatase β
563 (RPTPβ) activity and signaling are attenuated by glycosylation and subsequent cell
564 surface galectin-1 binding. J. Biol. Chem. **283:**33026-33035.

565 7. **Earl L, Bi S, Baum L.** 2010. N- and O-glycans modulate galectin-1 binding, CD45
566 signaling, and T cell death. J. Biol. Chem. **285:**2232-2244.
567
568 8. **Zondag GCM, Koningstein GM, Jiang Y, Sap Y, Moolenaar WH, Gebbink**
569 **MFBG.** 1995. Homophilic interactions mediated by receptor tyrosine phosphatases μ
570 and κ. J. Biol. Chem. **270:**14247-14250.
571
572 9. **Jiang G, den Hertog J, Hunter T.** 2000. Receptor-like protein tyrosine phosphatase
573 alpha homodimerizes on the cell surface. Mol. Cell Biol. **20:**5971-5929.
574
575 10. **Aricescu AR, Hon W, Siebold C, Lu W, van der Merwe PA.** 2006. Molecular
576 analysis of receptor protein tyrosine phosphatase μ-mediated cell adhesion. EMBO J.
577 **25:**701-712.
578
579 11. **Magistrelli G, Toma S, Isacchi A.** 1996. Substitution of two variant residues in the
580 protein tyrosine phosphatase-like PTP35/IA-2 sequence reconstitutes catalytic
581 activity. Biochem. Biophys. Res. Commun. **227:**581-588.
582
583 12. **Torii S.** 2009. Expression and function of IA-2 family proteins, unique
584 neuroendocrine-specific protein-tyrosine phosphatases. Endocrin. J. **56:**639-648.
585

13. **Solimena M, Dirkx R Jr, Hermel JM, Pleasic-Williams S, Shapiro JA, Caron L, Rabin DU.** 1996. ICA 512, an autoantigen of type I diabetes, is an intrinsic membrane protein of neurosecretory granules. EMBO J. **15:**2102-2114.

14. **Wasmeier C, Hutton JC.** 1996. Molecular cloning of phogrin, a protein-tyrosine phosphatase homologue localized to insulin secretory granule membranes. J. Biol. Chem. **271:**18161-18170.

15. **Gross S, Blanchetot C, Schepens J, Albet S, Lammers R, den Hertog J, Hendriks W.** 2002. Multimerization of the protein-tyrosine phosphatase (PTP)-like insulin dependent Diabetes Mellitus autoantigens IA-2 and IA-2β with receptor PTPs (RPTPs). J. Biol. Chem. **277:**48139-48145.

16. **Trajkovski M, Mziaut H, Schubert S, Kalaidzidis Y, Altkrüger A, Solimena M.** 2008. Regulation of insulin granule turnover in pancreatic β-cells by cleaved ICA512. J. Biol. Chem. **283:**33719-33729.

17. **Hermel JM, Dirkx R Jr, Solimena M.** 1999. Post-translational modifications of ICA512, a receptor tyrosine phosphatase-like protein of secretory granules. Eur. J. Neurosci. **11:**2609-2620.

18. **Primo ME, Klinke S, Sica MP, Goldbaum FA, Jakoncic J, Poskus E, Ermácora MR.** 2008. Structure of the mature ectodomain of the human receptor-type protein-tyrosine phosphatase IA-2. J. Biol.Chem. **283:**4674-4681.

19. **Primo ME, Jakoncic J, Noguera ME, Risso VA, Sosa L, Sica MP, Solimena M, Poskus E, Ermácora MR.** 2011. Protein-protein interactions in crystals of the human receptor-type protein tyrosine phosphatase ICA512 ectodomain. PLOS One **6:**e24191.

20. **Noguera ME, Primo ME, Sosa LN, Risso VA, Poskus E, Ermácora MR.** 2013. Biophysical characterization of the membrane-proximal ectodomain of the receptor-type protein-tyrosine phosphatase phogrin. Protein Pept Lett. **20:**1009-1017.

21. **Noguera ME, Primo ME, Jakoncic J, Poskus E, Solimena M, Ermácora MR.** 2014. X-ray structure of the mature ectodomain of phogrin. J Struct Funct Genomics (in press).

22. **Asfari M, Janjic D, Meda P, Li G, Halban PA, Wollheim CB.** 1992. Establishment of 2-mercaptoethanol-dependent differentiated insulin-secreting cell lines. Endocrinol. **130:**167-178.

23. **Mziaut H, Trajkovski M, Kersting S, Ehninger A, Altkrüger A, Lemaitre RP, Schmidt D, Saeger H, Lee M, Drechsel DN, Müller S, Solimena M.** 2006.

630 Synergy of glucose and growth hormone signalling in islet cells through ICA512 and
631 STAT5. Nat. Cell Biol. **8:**435-445.
632
633 24. **Ligtenberg MJ, Kruijshaar L, Buijs F, van Meijer M, Litvinov SV, Hilkens J.**
634 1992. Cell-associated episialin is a complex containing two proteins derived from a
635 common precursor. J. Biol. Chem. **267:**6171-6177.
636
637 25. **Bork P, Patthy L.** 1995. The SEA module: a new extracellular domain associated
638 with O-glycosylation. Protein Sci. **4:**1421-1425.
639
640 26. **Wreschner DH, McGuckin MA, Williams SJ, Baruch A, Yoeli M, Ziv R, Okun**
641 **L, Zaretsky J, Smorodisnky N, Keydar I, Neophytou P, Stacey M, Lin H,**
642 **Gordon S.** 2002. Generation of ligand-receptor alliances by "SEA" module-
643 mediated cleavage of membrane-associated mucin proteins. Protein Sci. **11:**698-706.
644
645 27. **Khatri IA, Wang R, Forstner JF.** 2003. SEA (sea-urchin sperm protein,
646 enterokinase and agrin)-module cleavage, association of fragments and membrane
647 targeting of rat intestinal mucin Muc3. Biochem. J. **372:**263-270.
648
649 28. **Jonckheere N, Skrypek N, Frénois F, Van Seuningen I.** 2013. Membrane-bound
650 mucin modular domains: From structure to function. Biochimie **95:**1077-1086.
651

652 29. **Ort T, Voronov S, Guo J, Zawalich K, Froehner SC, Zawalich W, Solimena, M.**
653 2001. Dephosphorylation of β2-syntrophin and Ca^{2+}/μ-calpain-mediated cleavage of
654 ICA512 upon stimulation of insulin secretion. EMBO J. **20:**4013-4023.
655
656 30. **Trajkovski M, Mziaut H, Altkrüger A, Ouwendijk J, Knoch K, Müller S,**
657 **Solimena M.** 2004. Nuclear translocation of an ICA512 cytosolic fragment couples
658 granule exocytosis and insulin expression in β-cells. J. Cell Biol. **167:**1063-1074.
659
660 31. **Julenius K, Molgaard A, Gupta R, Brunak S.** 2004. Prediction, conservation
661 analysis, and structural characterization of mammalian mucin-type O-glycosylation
662 sites. Glycobiology **15:**153-164.
663
664 32. **Bloomquist BT, Darlington DN, Mains RE, Eipper BA.** 1994. RESP18, a novel
665 endocrine secretory protein transcript, and four other transcripts are regulated in
666 parallel with pro-opiomelanocortin in melanotropes. J. Biol. Chem. **269:**9113-9122.
667
668 33. **Zhang G, Hirai H, Cai T, Miura J, Yu P, Huang H, Schiller MR, Swaim WD,**
669 **Leapman RD, Notkins AL.** 2007. RESP18, a homolog of the luminal domain of IA-
670 2, is found in dense core vesicles in pancreatic islet cells and is induced by high
671 glucose. J. Endocrinol. **195:**313-321.
672
673 34. **Gerdes H, Rosa P, Phillips E, Bauerle PA, Frank R, Argos P, Huttner WB.** 1989.
674 The primary structure of human secretogranin II, a widespread tyrosine-sulfated

675 secretory granule protein that exhibits low pH- and calcium-induced aggregation. J.
676 Biol. Chem. **264:**12009-120015.
677
678 35. **Thiele C, Gerdes H, Huttner WB.** 1997. Protein secretion: Puzzling receptors. Curr.
679 Biol. **7:**496-500.
680
681 36. **Glombik MM, Krömer A, Salm T, Huttner WB, Gerdes H.** 1999. The disulfide-
682 bonded loop of chromogranin B mediates membrane binding and directs sorting
683 from the trans-Golgi network to secretory granules. EMBO J. **18:**1059-1070.
684
685 37. **Saito N, Takeuchi T, Kawano A, Hosaka M, Hou N, Torii S.** 2011. Luminal
686 interaction of Phogrin with Carboxypeptidase E for effective targeting to secretory
687 granules. Traffic **12:**499-506.
688
689 38. **Schiller MR, Mains RE, Eipper BA.** 1995. A neuroendocrine-specific protein
690 localized to the endoplasmic reticulum by distal degradation. J. Biol. Chem.
691 **270:**26129-26138.
692
693 39. **Payton MA, Hawkes CJ, Christie MR.** 1995. Relationship of the 37,000- and
694 40,000-M_r tryptic fragments of islet antigens in insulin-dependent diabetes to the
695 protein tyrosine phosphatase-like molecule IA-2 (ICA512). J. Clin. Invest. **96:**1506-
696 1511.
697

698 40. **Notkins AL, Lu J, Li Q, VanderVegt FP, Wasserfall C, Maclaren NK, Lan MS.**
699 1996. IA-2 and IA-2β are major autoantigens in IDDM and the precursors of the 40
700 kDa and 37 kDa tryptic fragments. J. Autoimmunity **9:**677-682.
701

FIGURE LEGENDS

FIG 1 Sequence of the ICA512 extracellular domain and model of ME ICA512 dimerization through β2-β2 and β4-β4 interfaces. (A) Primary amino acid sequence of human ICA512 extracellular domain (amino acid residues 1-575), including the signal peptide (SP, residues 1-34), the RESP18 homology domain (RESP18-HD, residues 35-133), as a part of the N-terminal fragment (NTF, residues 35-448) and the mature ectodomain (ME, residues 449-575, in bold). Residues in α-helices and β-strands of ME ICA512, as resolved in (18) are highlighted in orange and yellow, respectively. The N-glycosylation sites N506 and N524 are indicated in red and cleavage sites for protein convertases (KR 132-133, KK 386-387 and KK 447-448) are underlined. Clustered cysteines within the RESP18-HD (C40, C47, C53 and C62) are indicated in italics, while threonines and serines predicted as putative *O*-glycosylation sites are indicated with asterisks. Critical residues for β2-β2 (S508) or β4-β4 (G553) mediated dimerization of recombinant ME ICA512 *in vitro* are shown in purple. (B) Modeled β2-β2 (left) or β4-β4 (right) ME ICA512 dimers (the symmetry axes shown by dotted lines), as resolved by X-ray crystallography (18). Color code for the relevant residues and secondary structures are as described in (A). Schematic drawing of ICA512 below shows the extracellular domain regions as in (A), followed by the transmembrane (TM) region and the cytosolic PTP domain. The arrow and arrowhead indicate the cleavage site for conversion of proICA512 into ICA512-TMF and the more distal cleavage site for calpain in the cytoplasmic domain of ICA512-TMF, respectively.

725 FIG 2 ME ICA512 is sufficient for dimerization of proICA512 in INS-1 cells. (A)
726 Schematic drawing of ICA512-GFP and ICA512-HA, and their detection by
727 immunoblotting with the mouse anti-GFP or rabbit anti-HA antibody in lysates of single
728 transfected INS-1 cells. The arrows indicate the cleavage site for conversion of
729 proICA512 into ICA512-TMF, while the arrowheads indicate the more distal calpain
730 cleavage site in the cytoplasmic domain of ICA512-TMF. Prior to lysis cells were kept
731 either at rest (R) in 0 mM glucose and 5 mM KCl or stimulated (S) for 2 hours either with
732 55 mM KCl (High K^+) or 25 mM glucose (High Glucose) or both (High Glucose and
733 High K^+, HGHK) ($n \geq 3$). (B) Immunoblottings for HA or GFP on lysates of INS-1 cells
734 transfected with ICA512-HA alone or together with ICA512-GFP. Prior to lysis the cells
735 were either kept at rest (R) or stimulated (S) for 2 hours with HGHK ($n \geq 3$). For
736 normalization, the same cell lysates were also immunoblotted for γ-tubulin. (C)
737 Immunoblottings for HA or GFP on immunoprecipitates with goat anti-GFP antibody or
738 goat IgG from the lysates shown in (B) ($n \geq 3$). (D) Schematic drawing of ME ICA512-
739 GFP and immunoblottings for HA or GFP on lysates and corresponding
740 immunoprecipitates with goat anti-GFP antibody from INS-1 cells transfected with
741 ICA512-HA alone or together with ME ICA512-GFP. Prior to lysis the cells were kept at
742 rest (R) or stimulated (S) for 2 hours with HGHK ($n \geq 3$). For normalization, the same cell
743 lysates were also immunoblotted for γ-tubulin.
744
745 FIG 3 Perturbing N-glycosylation or ME ICA512 β2-strand does not prevent ICA512
746 targeting to SGs. (A, B) Immunoblottings for GFP or ICA512 on lysates of resting (A) or
747 stimulated (B) INS-1 cells transfected either with ICA512-GFP wt or the mutants N506A,

N524A, N506A/N524A or S508A (n≥3). For normalization, the same cell lysates were also immunoblotted for γ-tubulin. (C) Quantification by ANOVA of proICA512-GFP species (top panel) and of the ratios of the corresponding proICA512-GFP/ICA512-TMF-GFP species (bottom panel). Values ± SEM for each ICA512 species were normalized to those of γ-tubulin in the same lysates; *, $p<0.005$ (n=3). (D) Confocal microscopy images of HGHK stimulated INS-1 cells transfected with ICA512-GFP or the corresponding N506A/N524A or S508A mutants (in green) and immunostained for insulin (in red) (n≥3). Nuclei were labeled with DAPI (in blue). Scale bars = 5 μm. (E) Levels of insulin mRNA in ICA512-GFP wt and ICA512-GFP N506A/N524A sorted cells as measured by RT-PCR and normalized for β-actin mRNA levels (n=3). Levels of (F) proinsulin and (G) insulin content in ICA512-GFP wt and ICA512-GFP N506A/N524A sorted cells kept at rest (R) or stimulated (S) for 2 hours with HGHK as measured by ELISA (n=3). (H) Insulin secretion measured from ICA512-GFP wt and ICA512-GFP N506A/N524A sorted cells kept at rest (R) or stimulated (S) for 2 hours with HGHK (n=3).

FIG 4 Perturbing the ME ICA512 β4-strand impairs proICA512 stability and targeting to SGs. (A, B) Immunoblottings for GFP on lysates of resting (R) or HGHK stimulated (S) INS-1 cells transfected with ICA512-GFP or ICA512-GFP G553D and untreated (-) or treated (+) with the protease inhibitors MG-115 (A) or calpeptin (B) (n≥3). For normalization, the same cell lysates were also immunoblotted for γ-tubulin. (C) Immunoblotting for GFP on lysates of HGHK stimulated INS-1 cells transfected with ICA512-GFP or ICA512-GFP G553D and untreated (-) or treated (+) with N-glycosidase PNGaseF (n≥3). (D) Confocal microscopy images of HGHK stimulated INS-1 cells

771 transfected with ICA512-GFP (top panels) or the corresponding G553D mutant (bottom
772 panels), and immunostained for insulin (in red, left panels) or co-labeled with the ER
773 tracker red (in red, right panels) (n≥3). Nuclei were labeled with DAPI (in blue). Scale
774 bars = 5 µm.
775
776 FIG 5 ME ICA512 is *O*-glycosylated. (A) Ponceau S staining of recombinant fetuin
777 untreated (-) or treated (+) with *O*-glycosidases. (B) Immunoblottings for GFP on lysates
778 of resting (R) or HGHK stimulated (S) INS-1 cells transfected with ICA512-GFP,
779 ICA512-GFP N506A, ICA512-GFP S508A or ICA512-GFP G553D, untreated (-) or
780 treated (+) with *O*-glycosidases (n≥3). (C) Immunoblotting for ICA512 on lysates of
781 resting (R) or HGHK stimulated (S) mouse and human pancreatic islets, untreated (-) or
782 treated (+) with *O*-glycosidases (upper and lower panels, n=3 and n=2, respectively). For
783 normalization, the same lysates were also immunoblotted for γ-tubulin. (D)
784 Immunoblottings for GFP on lysates of HGHK stimulated INS-1 cells transfected with
785 ME ICA512-GFP, ME ICA512-GFP S508A or ME ICA512-GFP G553D, untreated (-)
786 or treated (+) with *O*-glycosidases, PNGaseF or Endoglycosidase H (n=3). (E) Merge
787 confocal microscopy images of INS-1 cells transfected with ME ICA512-GFP or ME
788 ICA512-GFP G553D (in green) and co-labeled with the ER tracker red (in red) and DAPI
789 for nuclei (in blue) (n=3). Scale bars = 10 µm. (F) Schematic drawing of ICA512-GFP
790 ΔNTF, and immunoblotting for GFP on lysates of HGHK stimulated INS-1 cells
791 transfected with ICA512-GFP ΔNTF, ICA512-GFP ΔNTF S508A or ICA512-GFP ΔNTF
792 G553D, untreated (-) or treated (+) with *O*-glycosidases, PNGaseF or Endoglycosidase H

(n=3). Fetuin (A) and the ICA512 related protein fragments (B, C, F) sensitive to *O*-glycosidase treatment (+) are indicated by arrowheads (<).

FIG 6 NTF targets ICA512 to SGs. (A-C) Confocal microscopy images of resting (A, B) or HGHK stimulated (C) INS-1 cells transfected with ICA512-GFP (top panels, green) or ICA512-GFP ΔNTF (bottom panels, green). Live cells were incubated at 4 °C with the mouse anti-ME ICA512 antibody (A, C) together with the guinea pig anti-insulin antibody (A), and also alternatively with the mouse anti-ICA512 CT antibody (B). After fixation, the binding of the primary antibodies to the cell surface was detected by incubation with Alexa-conjugated anti-mouse (A, B, C; in red) or anti-guinea pig (A; in white) IgGs. Merge images are additionally shown for (A) and (C). Scale bars = 10 μm (n≥3). (D, E) Immunoblottings for GFP (D) and ME ICA512 (E) on lysates of resting (R) or HGHK stimulated (S) INS-1 cells transfected with ICA512-GFP or ICA512-GFP ΔNTF (n≥3). For normalization, the same lysates were also immunoblotted for γ-tubulin.

FIG 7 NTF contains information for both ER retention and SG targeting. (A) Schematic drawing of ICA512-RESP18-HD-GFP, and confocal microscopy images of resting INS-1 cells transfected with ICA512-RESP18-HD-GFP (in green) and immunostained for insulin (in red) (n≥3). Nuclei were labeled with DAPI (in blue). Scale bars = 5 μm. (B) Immunoblottings for GFP on lysates (left panel) or immunoprecipitates obtained with a different, goat anti-GFP antibody from incubation media (right panel) of resting (R) and HGHK stimulated (S) INS-1 cells transfected with ICA512-RESP18-HD-GFP (n≥3). The cell lysates were immunoblotted also for γ-tubulin. (C, D) Schematic drawing of ICA512-

NTF-GFP, and confocal microscopy images of resting INS-1 cells transfected with ICA512-NTF-GFP (in green), and immunostained for insulin (C, in red) or calnexin (D, in red) (n≥3). Nuclei were labeled with DAPI (in blue). Scale bars = 5 µm. (E) Immunoblottings for GFP (left panel) or NTF (right panel), on lysates of INS-1 cells transfected with either CD33-GFP or ICA512-NTF-GFP (lanes 1 vs. 2) (n≥3). (F) Schematic drawing of ICA512-NTF, and confocal microscopy images of INS-1 cells transfected with ICA512-NTF, and immunostained for NTF (in green) and calnexin (in red) (n≥3). Scale bars = 5 µm.

FIG 8 Establishment of ME ICA512 β4-β4 dimers overcome the NTF ER retention signal. (A) Immunoblottings for GFP (top panel) or HA (bottom panel) in the lysates of HGHK stimulated INS-1 cells transfected with ICA512-HA alone (lane 1) or double transfected with ICA512-HA and ME ICA512-GFP (lane 2) or with the respective ICA512-HA and ME ICA512-GFP mutants S508A, G553D, S508A/G553D or N506A/G553D (lanes 3-6) (n≥3). (B) Immunoblottings for GFP (top panel) or HA (bottom panel) on immunoprecipitates obtained with goat anti-GFP antibody (lanes 7-12) or control IgG (lanes 13-18) from the corresponding cell lysates shown in (B) (n≥3). (C) Quantification of the immunoprecipitates in (B), for all comparisons (n=5), $p<0.05$, *. (D) Immunoblottings for HA on Endoglycosidase H or PNGaseF untreated (-) or treated (+) lysates from resting (top panel) or HGHK stimulated (bottom panel) INS-1 cells transfected with ICA512-HA, ICA512-HA S508A, G553D or S508A/G553D (n≥3). (E) Model on how N506 glycosylation affects the folding and dimerization of ME ICA512 β2-β2 and β4-β4 association interfaces and the export of proICA512 from the ER.

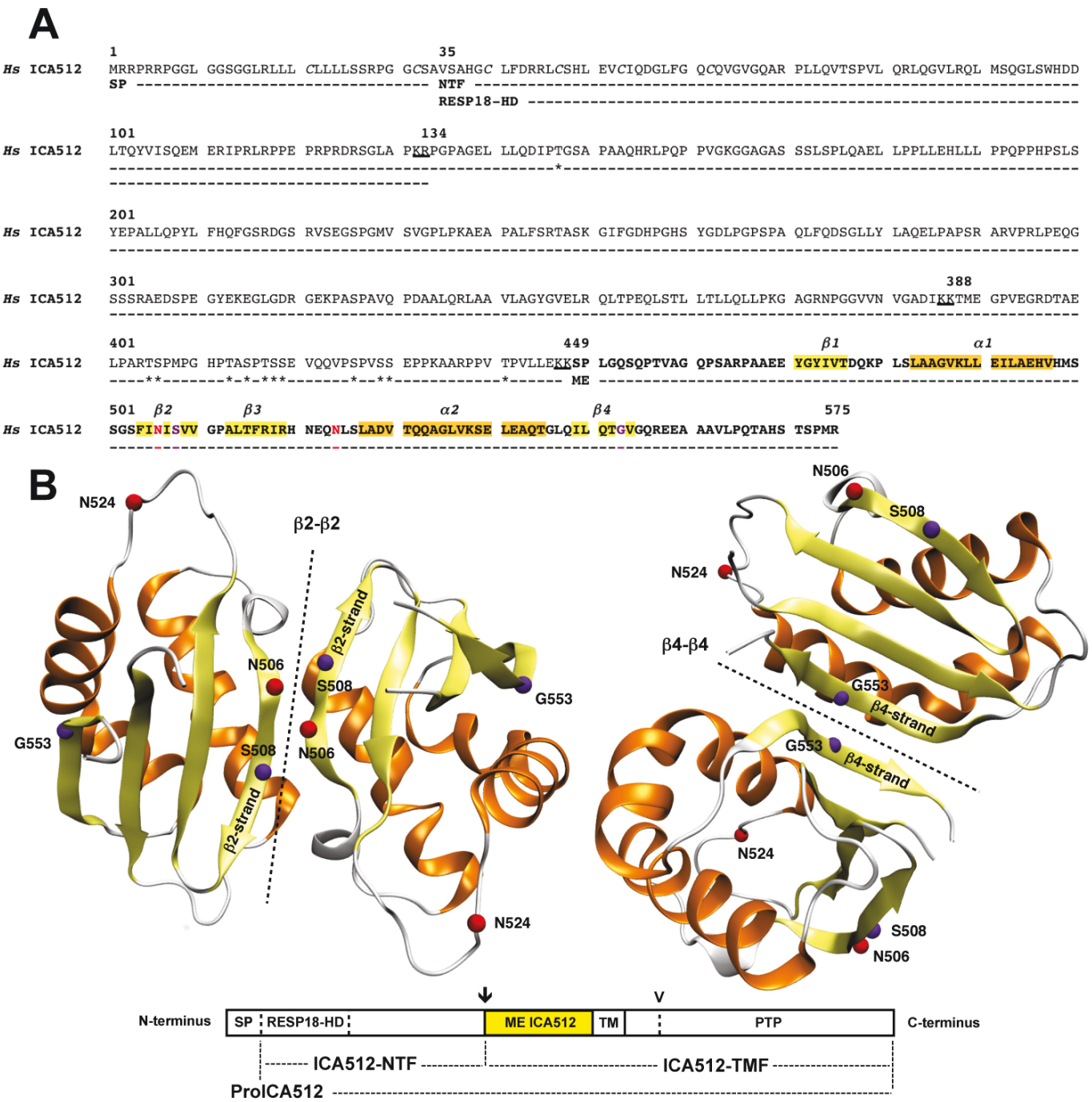

FIG 1 Torkko et al. 2014

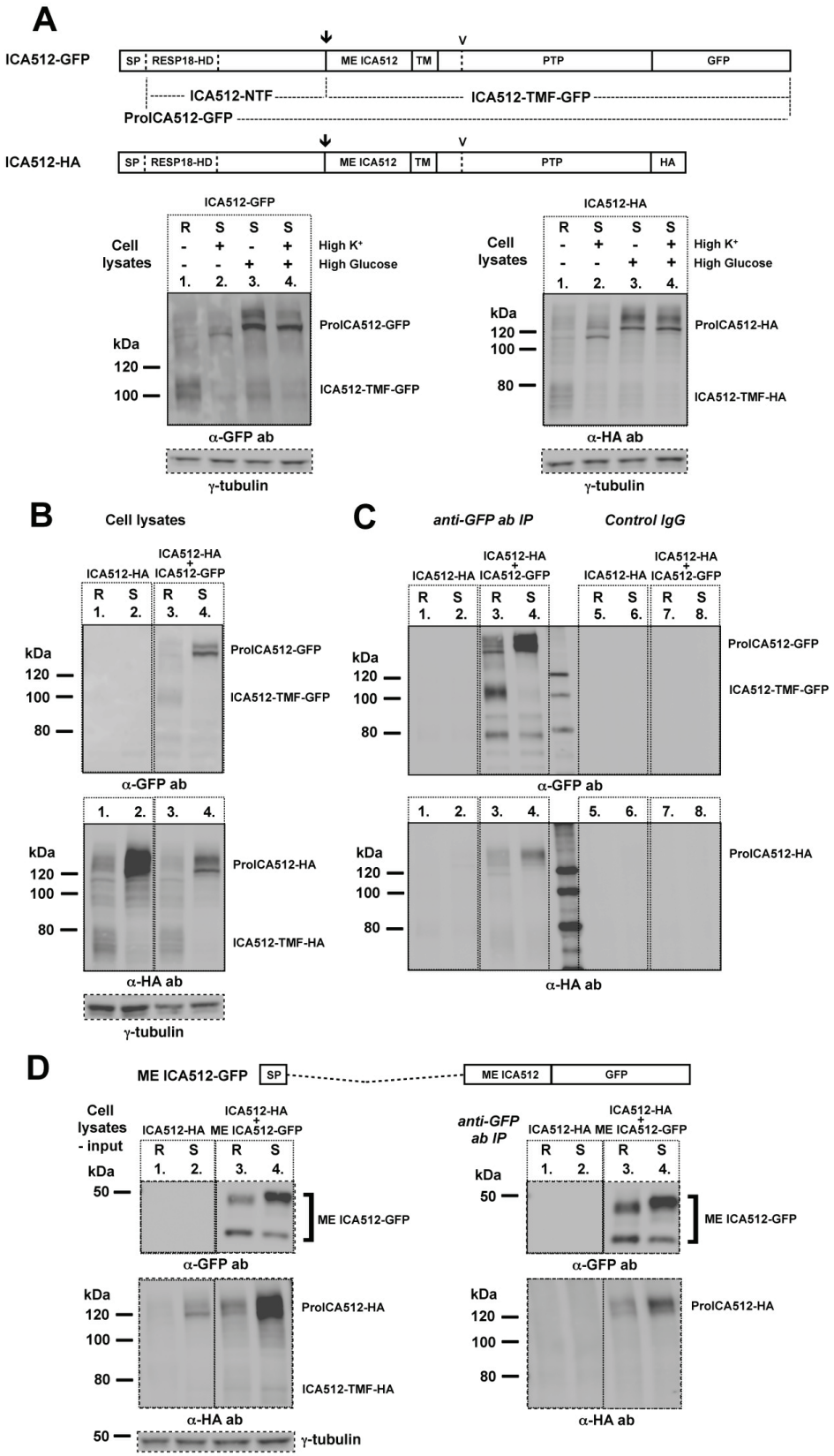

FIG 2 Torkko et al. 2014

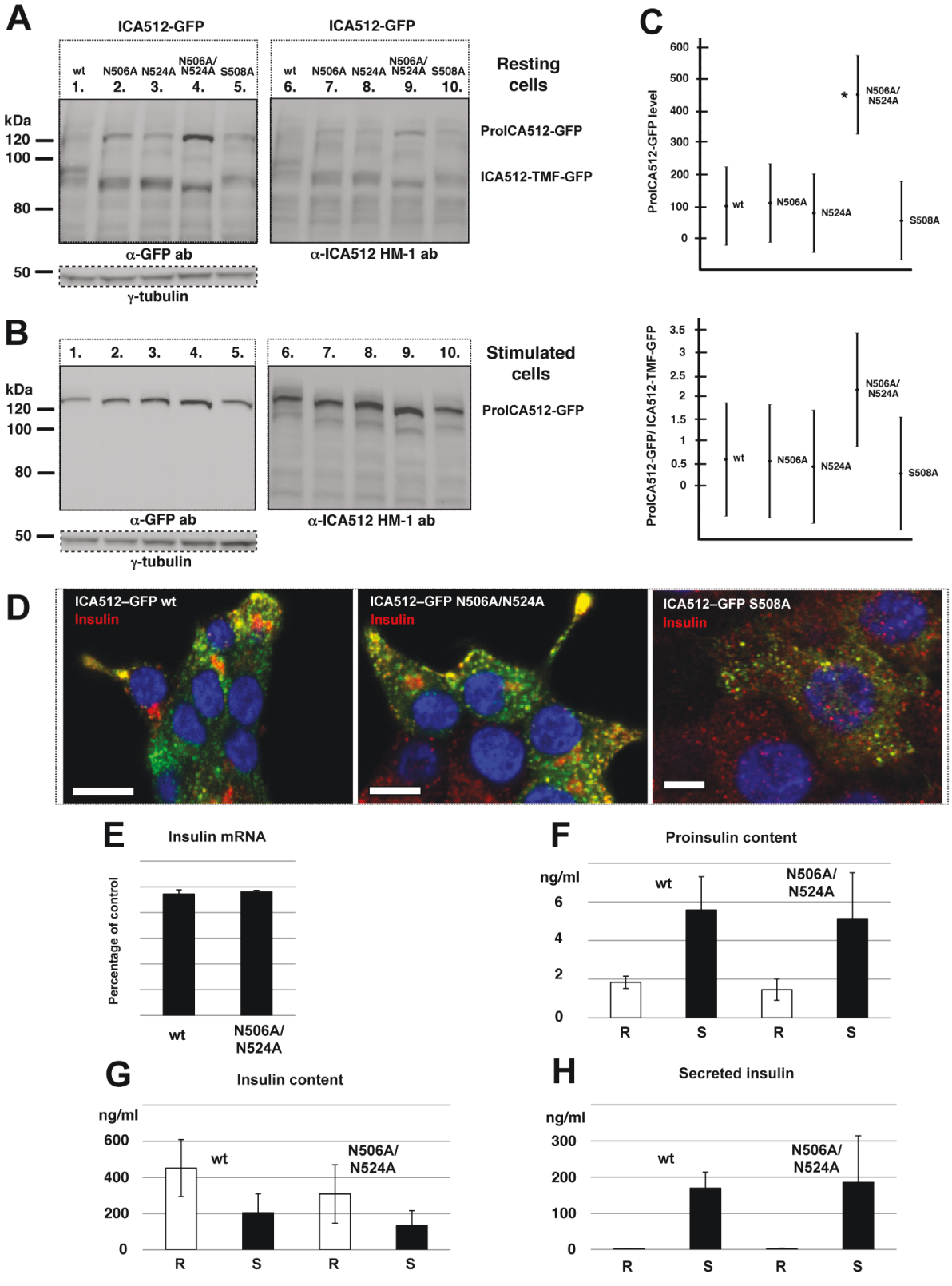

FIG 3 Torkko et al. 2014

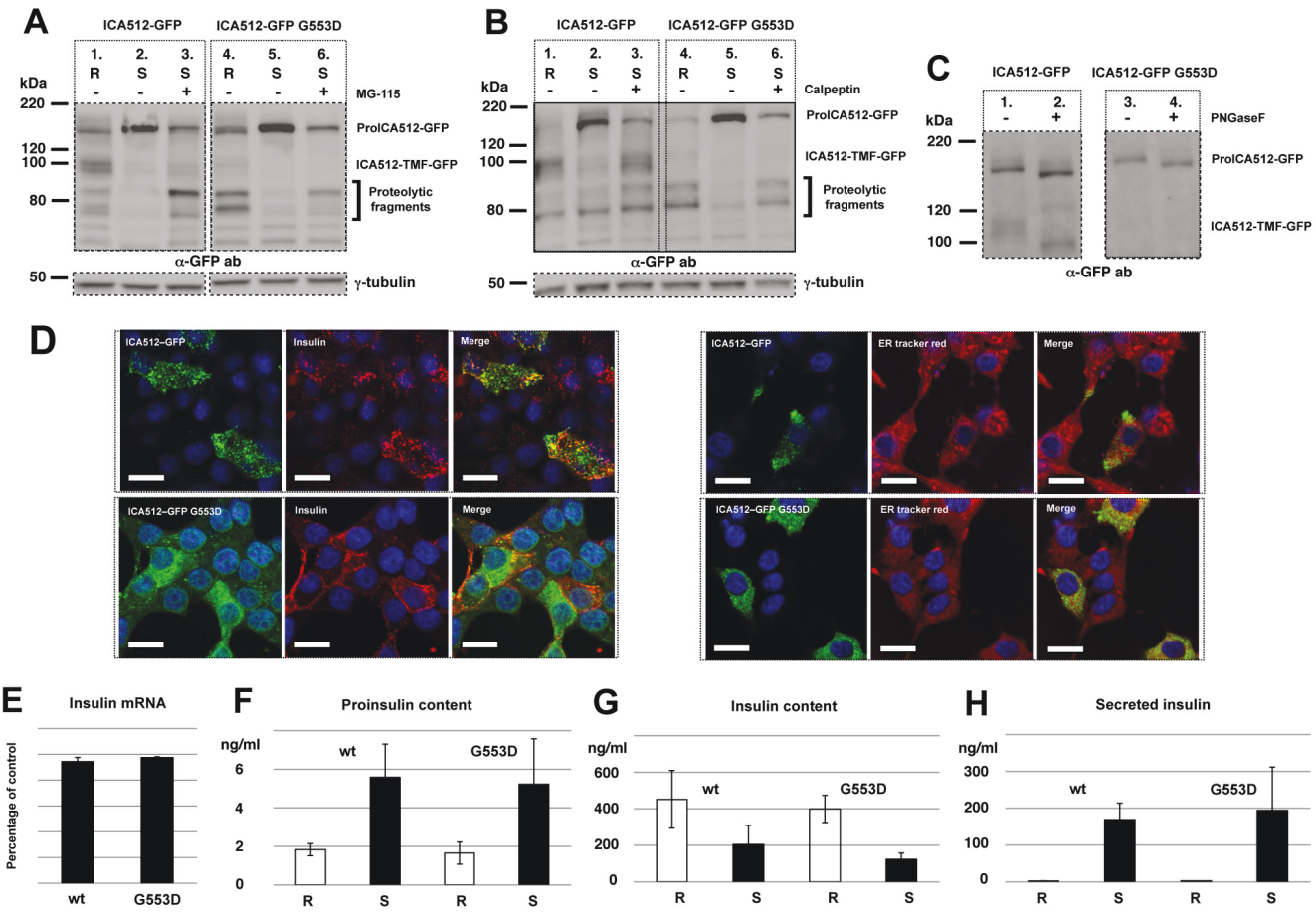

FIG 4 Torkko et al. 2014

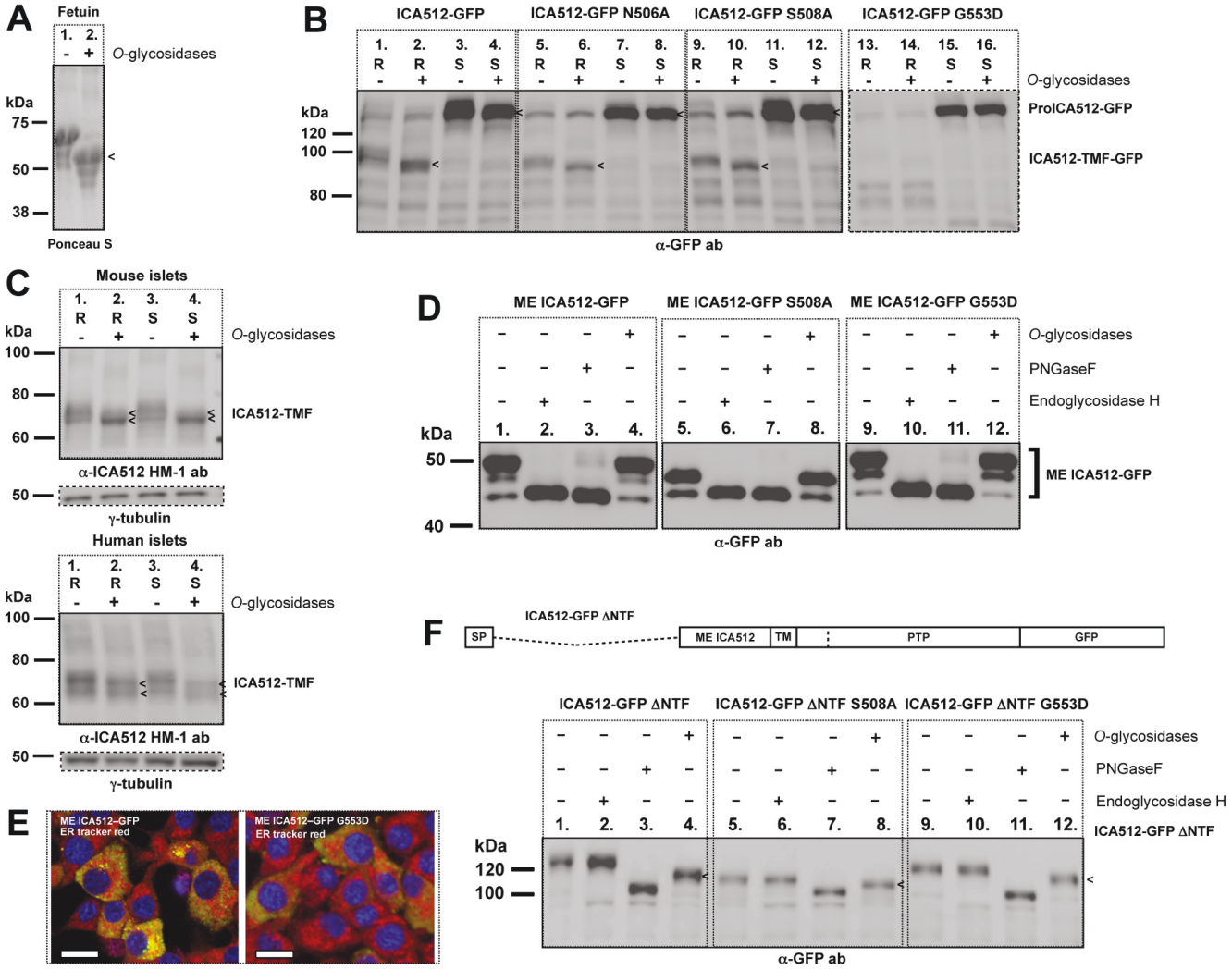

FIG 5 Torkko et al. 2014

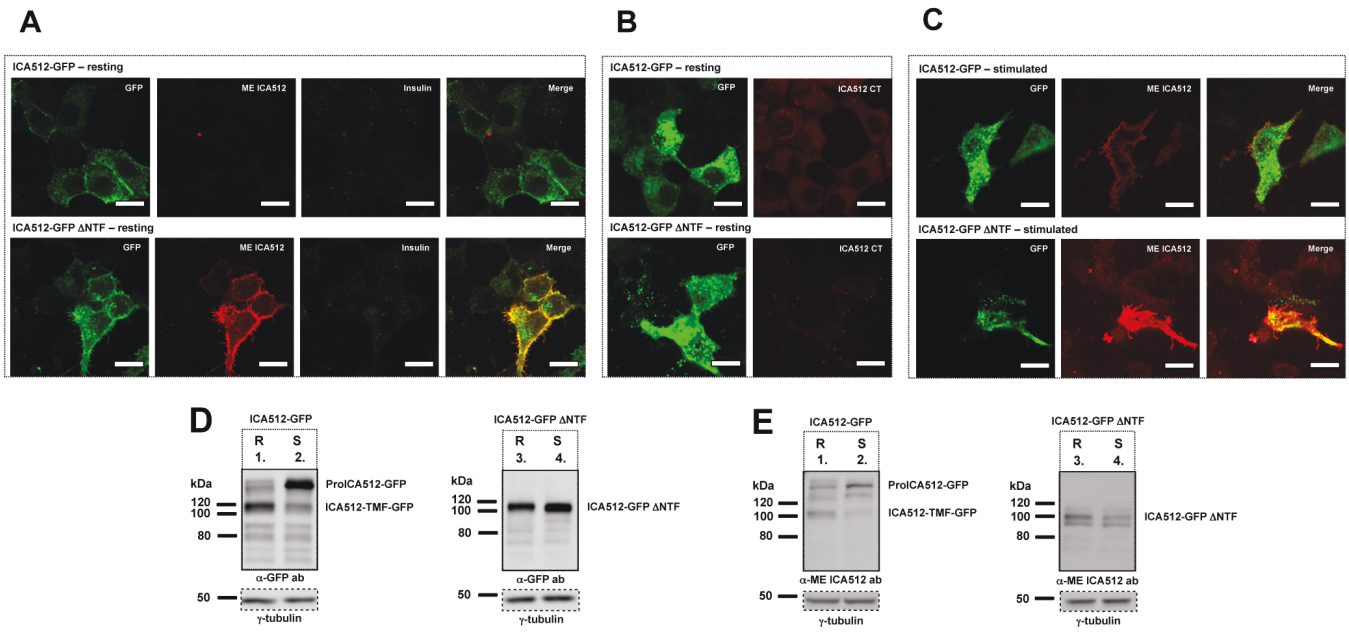

FIG 6 Torkko et al. 2014

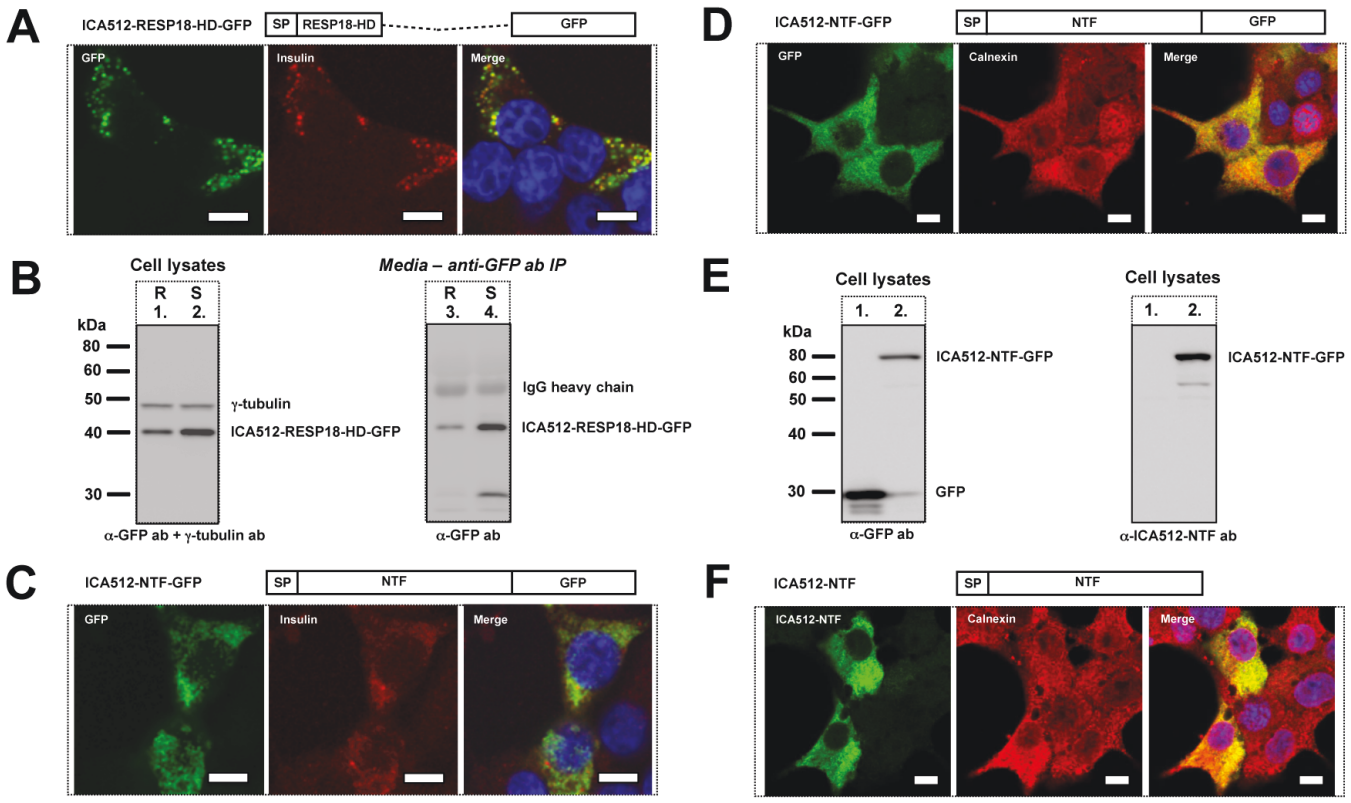

FIG 7 Torkko et al. 2014

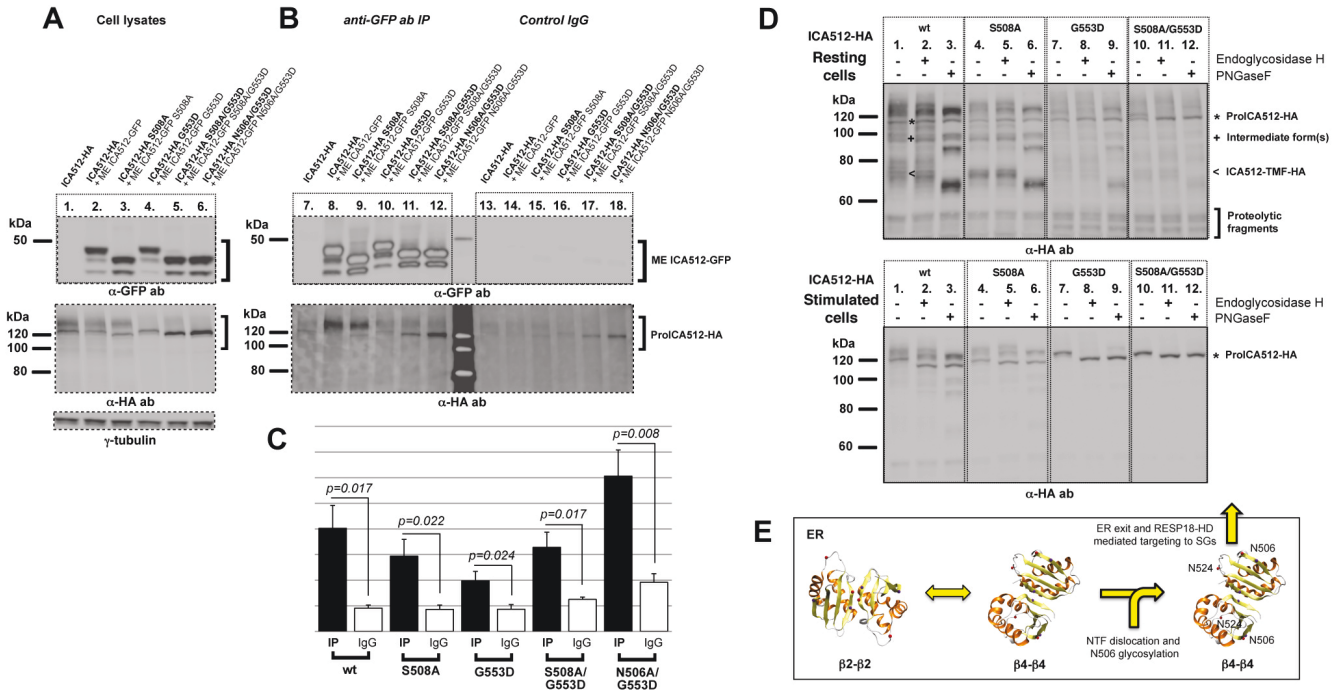

FIG 8 Torkko et al. 2014